

Modelling infiltration by means of a nonlinear fractional diffusion model

E Gerolymatou¹, I Vardoulakis¹ and R Hilfer^{2,3}

¹ Department of Mechanics, Faculty of Applied Mathematics and Physics, N.T.U. Athens, 9 Iroon Politechneiou Street, 15780 Athens, Greece

² Institute for Computational Physics, Universität Stuttgart, Pfaffenwaldring 27, 70569 Stuttgart, Deutschland

³ Institut für Physik, Universität Mainz, 55099 Mainz, Deutschland

E-mail: eleni@mechan.ntua.gr

Received 18 May 2006, in final form 11 July 2006

Published 1 September 2006

Online at stacks.iop.org/JPhysD/39/4104

Abstract

The classical Richards equation describes infiltration into porous soil as a nonlinear diffusion process. Recent experiments have suggested that this process exhibits anomalous scaling behaviour. These observations suggest generalizing the classical Richards equation by introducing fractional time derivatives. The resulting fractional Richards equation with appropriate initial and boundary values is solved numerically in this paper. The numerical code is tested against analytical solutions in the linear case. Saturation profiles are calculated for the fully nonlinear fractional Richards equation. Isochrones and isosaturation curves are given. The cumulative moisture intake is found as a function of the order of the fractional derivative. These results are compared against experiment.

1. Introduction

A macroscopic theory for capillary flow through porous media has been a longstanding challenge in physics and engineering [1, 2]. Some of the key obstacles have been the incorporation of hysteresis and the prediction of residual saturations [3]. Recently macroscopic equations were found that overcome some of these obstacles [4–7]. In the present paper a different line of thought is followed.

The focus of this paper is on air–water flow through the unsaturated zone in soils. This hydrological system is traditionally described by the Richards equation [8]. This equation is closely related to the traditional macroscopic theory of two-phase flow [9]. Observations of anomalous diffusive behaviour during infiltration of building materials [10–12] and the similarity between the Richards equation and nonlinear diffusion suggest generalizing the Richards equation by introducing fractional time derivatives [13, 14].

The objective of this paper is to investigate the Richards equation with fractional time derivative numerically. In section 2 the fractional Richards equation is established by generalizing its classical formulation. In section 3 the numerical method to solve the equation is presented. In section 4 the numerical code is tested by comparison of the numerical solutions with analytical solutions for the linear

case. Finally the numerical results for the nonlinear fractional Richards equation are given and discussed in section 5.

2. Fractional Richards equation

2.1. Classical Richards equation

The present work is concerned with moisture movement in one-dimensional horizontal soil columns. Gravity is neglected. The case examined is presented in figure 1. At time $t = 0$ a wetting sponge is brought into contact with the soil column and the imbibition process begins. The volumetric moisture content $\theta(t, x)$, also called local volume fraction of water, is defined as the ratio of the volume of water to the volume of a representative elementary soil volume located at macroscopic position x . If ϕ is the interconnected porosity and S is the degree of water-saturation, then

$$\theta = \phi S. \quad (1)$$

For $\phi = \text{const.}$, the volumetric moisture content can be used instead of the degree of saturation S .

Under the assumptions that the porosity is constant (the soil skeleton is rigid) and that mass transfer between the

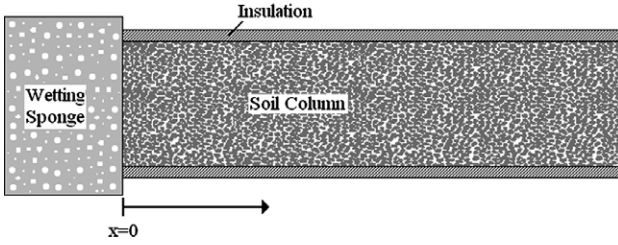


Figure 1. Horizontal soil column subjected to wetting.

aqueous and gaseous phases is negligible, mass balance yields

$$\frac{\partial \theta}{\partial t} = -\frac{\partial q}{\partial x}, \quad (2)$$

where q is the specific discharge of fluid through the interstices of the solid matrix. The fluid discharge in unsaturated media is determined, according to the generalized Darcy law, as

$$q = -K(\theta) \frac{\partial \Psi}{\partial x}, \quad (3)$$

where $\Psi(\theta(t, x))$ is the capillary potential per unit weight of water, defined as the work required to move a unit mass of water from a free-water surface to a specific point in the soil. Combining (2) and (3) yields

$$\frac{\partial \theta}{\partial t} = \frac{\partial}{\partial x} \left(C(\theta) \frac{\partial \theta}{\partial x} \right), \quad (4)$$

where $\theta(t, x)$ is defined on the nonnegative half-axis $x \geq 0$ and for $t \geq 0$.

$$C(\theta) = K(\theta) \frac{d\Psi}{d\theta}$$

is the moisture diffusivity, which is in general a function of the volumetric moisture content. For the moisture diffusivity the symbol D is often used. Here it is substituted by C to avoid confusion, because the same symbol is also used for derivatives of arbitrary order, which will be introduced later. Equation (4) is known as the Richards equation [8] and it is frequently used for the description of infiltration processes [15–17].

The initial condition is

$$\theta(0, x) = \begin{cases} \theta_1 & \text{if } x = 0 \\ \theta_0 & \text{if } x > 0 \end{cases} \quad (5)$$

and the boundary conditions read

$$\theta(t, 0) = \theta_1 \quad \text{for } t > 0, \quad x = 0 \quad (6)$$

and

$$\theta(t, x) < \infty \quad \text{for } t > 0, \quad x \rightarrow \infty, \quad (7)$$

where θ_0 and θ_1 are constants. The diffusivity $C(\theta)$ is given by a number of authors [18–21] as an exponential function of θ :

$$C(\theta) = C_0 \exp(c\theta), \quad (8)$$

where C_0 and c are constants. In what follows, the above function will be used for the classical Richards equation. This is one of many possible models and will be used here as an application example. Other models, see [22], could be equally well implemented. The values $C_0 = 4 \times 10^{-6} \text{ cm}^2 \text{ min}^{-1}$ and $c = 13.6$ from experiments on light Yolo clay conducted by Philip [23] will be used in the numerical calculations below.

2.2. Fractional generalization of Richards equation

Introducing the similarity variable

$$\xi = xt^{-1/2} \quad (9)$$

the Richards equation transforms into an ordinary differential equation. This fact can be used to find analytical solutions for soil water flow problems and also to find the dependence of the hydraulic conductivity on the volumetric moisture content [24]. However, in many cases significant deviations from the scaling law (9) have been reported [10–12]. These observations suggest a modified similarity variable of the form

$$\xi = xt^{-\alpha/2}, \quad (10)$$

where $\alpha < 1$ will be considered here.

The basic idea of generalizing the Richards equation consists in replacing the time derivative $\partial/\partial t$ in (4) with a fractional derivative of order α . This replacement introduces the scaling given by (10) into the Richards equation. That suggests to write an equation of the form

$$D^\alpha(\theta) = \frac{\partial}{\partial x} \left(C_\alpha(\theta) \frac{\partial \theta}{\partial x} \right), \quad (11)$$

where the fractional derivative D^α needs to be defined more precisely. A two parameter family of fractional derivatives of order $0 < \alpha \leq 1$ and type $0 \leq \beta \leq 1$ with respect to t was defined in [25] as

$$D_{a+}^{\alpha, \beta} f(t) = \left(I_{a+}^{\beta(1-\alpha)} \frac{d}{dt} \left(I_{a+}^{(1-\beta)(1-\alpha)} f \right) \right) (t) \quad (12)$$

for functions for which the expression on the right-hand side exists. The symbol $I_{a+}^\alpha f(t)$ stands for the fractional integral of order α of the function $f(t)$. It is defined as

$$I_{a+}^\alpha f(t) = \frac{1}{\Gamma(\alpha)} \int_a^t (t-u)^{\alpha-1} f(u) du. \quad (13)$$

The type β allows one to interpolate between the Riemann–Liouville derivative ($\beta = 0$) and the so-called Caputo–Liouville derivative ($\beta = 1$) (see [25, 26] for details). The problem of generalizing standard equations of motion by introducing fractional time is discussed in detail in [25] from a fundamental point of view. Here the fractional generalization of the Richards equation is postulated as a phenomenological equation of the form of (16) below. Note that (16), given below, has not been derived from pore scale equations, as has been done in [2]. Consequently, there is no relation between α and other hydraulic parameters.

The question of which type of fractional derivative to introduce is far from trivial. As shown in [25, 27] there is no reason to assume a derivative of type $\beta = 1$. Note also that [14] introduces a derivative of type $\beta = 0$, leading to problems with the initial condition [13]. Here we avoid the question by reformulating the classical Richards equation as an integral equation:

$$\theta(t, x) = \theta(0, x) + \int_0^t \frac{\partial}{\partial x} \left(C(\theta) \frac{\partial \theta}{\partial x} \right) dt \quad (14)$$

or

$$\theta(t, x) = \theta(0, x) + I_{0+}^1 \frac{\partial}{\partial x} \left(C(\theta) \frac{\partial \theta}{\partial x} \right), \quad (15)$$

where $\theta(0, x)$ is the initial condition. Substituting the integral on the right-hand side with a fractional integral of order $0 < \alpha \leq 1$ results in

$$\theta(t, x) = \theta(0, x) + I_{0+}^\alpha \frac{\partial}{\partial x} \left(C_\alpha(\theta) \frac{\partial \theta}{\partial x} \right). \quad (16)$$

Now the function $C_\alpha(\theta)$ is the fractional diffusivity and it is again assumed to be dependent on θ . The dependence of the diffusivity on α reflects the fact that its dimensions are

$$[C_\alpha] = L^2 T^{-\alpha} (0 < \alpha < 1). \quad (17)$$

From this point on (16) is referred to as the fractional Richards equation.

The same form of function as shown in (8) for the diffusivity will be used for the fractional diffusivity, namely:

$$C_\alpha(\theta) = C_{\alpha,0} \exp(c\theta). \quad (18)$$

In the absence of direct measurements the same numerical values are used for the constants, namely $C_{\alpha,0} = 4 \times 10^{-6} \text{ cm}^2 \text{ min}^{-\alpha}$ and $c = 13.6$. As initial and boundary condition the ones given in (5), (6) and (7) will be used.

Because the retention function and hydraulic conductivity show hysteresis, the moisture diffusivity will in general also be hysteretic. This can be incorporated into the fractional model in the same way as its usually done for $\alpha = 1$. In an analogous way effects of macroscopic heterogeneity can be included by allowing a position-dependent moisture diffusivity.

A microscopic explanation for the appearance of fractional time derivatives for linear or nonlinear diffusion was first given in [28] in terms of an underlying random walk model. Microscopically, the slow temporal decay is caused by strong fluctuations in the waiting time between events. In the random walk interpretation of the Richards equation the microscopic events correspond to snapoff and coalescence of interfaces mainly in the region of the capillary fringe. For a thorough discussion and overview of the underlying microscopic random walk interpretation of linear or nonlinear diffusion see also [25] and [27].

2.3. Previous work

In [14], following the scaling deviations observed in experiments from the scaling resulting from the Richards equation (cf table 1 of [23]) the following equation was considered:

$$D_{0+}^{\alpha,0} \theta = \frac{\partial}{\partial x} \left(C_\alpha(\theta) \frac{\partial \theta}{\partial x} \right), \quad (19)$$

replacing the derivative with respect to time with a fractional one. Consequently a solution of the resulting time-fractional absorption equation was attempted by inserting the similarity variable from (10) and transforming the equation into an ordinary differential equation, as was done by Philip, who introduced the similarity transform in the Richards equation. In an attempt to reproduce the results, we found that the transformation of (19) into an ordinary fractional differential equation is not possible in the same way as in the case $\alpha = 1$.

This is because the authors assumed the following relationship to hold:

$$D_{0+}^{\alpha,0} \theta = \frac{d\theta}{d\xi} D_{0+}^{\alpha,0} \xi, \quad (20)$$

which leads to the ordinary fractional differential equation:

$$\frac{d}{d\xi} \left(C_\alpha(\theta) \frac{d\theta}{d\xi} \right) - \frac{\Gamma(1 - \alpha/2)}{\Gamma(1 - 3\alpha/2)} \xi \frac{d\theta}{d\xi} = 0. \quad (21)$$

Let us assume as a counter example that $\theta = t^a, \xi = t^b$. Then, for (20) to hold the following relationship should hold for all values of b :

$$z(b) = \frac{1}{b} \frac{\Gamma(1 + b)}{\Gamma(1 + b - a)} = \text{const.} \quad (22)$$

However, this is not true. This finding gives rise to serious doubts concerning the validity of the numerical solution presented in [14]. An additional implication is the fact that, as already mentioned, the equation considered would in fact require an initial condition of integral type, which is not provided and in experimental situations is hard to obtain. Note also that the formulation of [14] (equation (19)) violates probability conservation while our formulation (equation (16)) does not.

3. Numerical method

For the solution of (16) an Adams–Bashforth–Moulton algorithm is used [29], modified slightly for nonlinearity. Equation (16) is a weakly-singular Volterra equation of the second type:

$$\theta(t, x) = \theta(0, x) + \frac{1}{\Gamma(\alpha)} \int_0^t (t - u)^{\alpha-1} \frac{\partial}{\partial x} \left(C_\alpha(\theta) \frac{\partial \theta}{\partial x} \right) du. \quad (23)$$

Considering an equidistant mesh with respect to time, with step equal to h , the numerical solution is given by the equation

$$\begin{aligned} \theta_{n+1}(x) = \theta(0, x) + \frac{1}{\Gamma(\alpha)} \left(\sum_{j=0}^n a_{j,n+1} F(t_j, x, \theta_j(x)) \right. \\ \left. + a_{n+1,n+1} F(t_{n+1}, x, \theta_{n+1}(x)) \right). \end{aligned} \quad (24)$$

This is nonlinear and, as a result, is solved by means of the iterative Newton–Raphson method [30, 31]. As initial point for the Newton–Raphson method the predictor $\theta_{n+1}^P(x)$ is used, evaluated by the relationship

$$\theta_{n+1}^P(x) = \theta(0, x) + \frac{1}{\Gamma(\alpha)} \sum_{j=0}^n b_{j,n+1} F(t_j, x, \theta_j(x)), \quad (25)$$

where

$$F(t, x, \theta) = \frac{\partial}{\partial x} \left(C_\alpha(\theta) \frac{\partial \theta}{\partial x} \right).$$

Note that the evaluation of the sought function at some instant of time requires knowledge of the complete past history. This reflects the nonlocality of fractional derivatives. The indices in the equations of the present section are integers and signify the

points of the mesh. The weights of integration are evaluated as follows for the predictor formula:

$$b_{j,n+1} = \frac{h^\alpha}{\alpha} ((n+1-j)^\alpha - (n-j)^\alpha),$$

while for the corrector formula

$$a_{0,n+1} = \frac{h^\alpha}{\alpha(\alpha+1)} (n^{\alpha+1} - (n-\alpha)(n+1)^\alpha)$$

$$a_{n+1,n+1} = \frac{h^\alpha}{\alpha(\alpha+1)},$$

and for $1 \leq j \leq n$

$$a_{j,n+1} = \frac{h^\alpha}{\alpha(\alpha+1)} ((n-j+2)^{\alpha+1} + 2(n-j+1)^{\alpha+1} + (n-j)^{\alpha+1}).$$

With respect to space finite elements with quadratic basis functions are used.

The initial conditions resulting from setting $\theta_1 = 0.5$ and $\theta_0 = 0.1$ are used. Furthermore, (8) and (18) are used in the calculations that follow.

4. Verification of the numerical code

In this section the numerical code is checked by comparing with analytical results for both $\alpha = 1$ and $\alpha < 1$ of the linear classical and fractional equations, (26) and (27), respectively,

$$\theta(t, x) = \theta(0, x) + C_1 I_{0+}^1 \frac{\partial^2 \theta}{\partial x^2}, \quad (26)$$

$$\theta(t, x) = \theta(0, x) + C_\alpha I_{0+}^\alpha \frac{\partial^2 \theta}{\partial x^2}, \quad (27)$$

where C_1 and C_α are constant diffusion coefficients. For the diffusion coefficients C_1 and C_α the values $C_1 = 24 \times 10^{-5} \text{ cm}^2 \text{ min}^{-1}$ and $C_\alpha = 24 \times 10^{-5} \text{ cm}^2 \text{ min}^{-\alpha}$, corresponding approximately to $\theta = 0.3$ in (8) and (18), respectively, are used.

4.1. Classical diffusion

The analytical solution of (26) is

$$\theta(t, x) = B_1 \cdot \text{erfc} \left(\sqrt{\frac{x^2}{4C_1 t}} \right) + B_2 \quad (28)$$

as may be verified by inserting the analytic solution into the equation. For the initial and boundary values we chose $\theta_0 = 0.1$ and $\theta_1 = 0.5$ and this fixes the constants B_1 and B_2 as

$$B_1 = 0.4, \quad B_2 = 0.1. \quad (29)$$

The volumetric moisture content as a function of the similarity variable $\xi = x/t^{1/2}$ was evaluated for both the numerical and the analytical results. The maximum difference between the numerical and the analytical solution is equal to 8.7×10^{-6} .

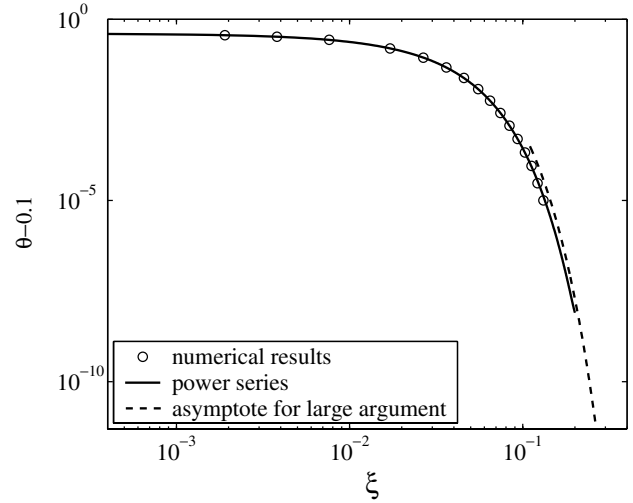


Figure 2. Numerical solution and asymptote for large argument of the analytical solution of the fractional linear diffusion equation.

4.2. Anomalous diffusion

For (27) the analytical solution is

$$\theta(t, x) = B_3 \cdot H_{1,1}^{1,0} \left(\sqrt{\frac{x^2}{C_\alpha t^\alpha}} \middle| \begin{matrix} (1, \alpha/2) \\ (0, 1) \end{matrix} \right) + B_4 \quad (30)$$

where $H_{1,1}^{1,0}(z)$ is the Fox function [32] defined by the series

$$H_{1,1}^{1,0} \left(z \middle| \begin{matrix} (1, \alpha/2) \\ (0, 1) \end{matrix} \right) = \sum_{v=0}^{\infty} \frac{1}{\Gamma(1 - \alpha v/2)} \frac{(-1)^v z^v}{v!}. \quad (31)$$

For $\alpha = 1$ this reduces to the complementary error function. Again we chose $\theta_0 = 0.1$ and $\theta_1 = 0.5$ to get

$$B_3 = 0.4, \quad B_4 = 0.1. \quad (32)$$

The fact that $\theta(t, x)$ given by (30) and (31) is the solution of (27) can be verified directly by inserting the analytic solution into equation (27).

For $z \rightarrow \infty$, again according to [32], any Fox function with $n = 0$ can be written in the form of an exponentially small series. Keeping only the first term of the series

$$H_{1,1}^{1,0} \left(z \middle| \begin{matrix} (1, \alpha/2) \\ (0, 1) \end{matrix} \right) \approx \frac{e}{\sqrt{\pi \alpha}} (\beta \mu^\mu z)^{-1/2\mu} \times \exp \left(-(\beta \mu^\mu z)^{1/\mu} \right), \quad (33)$$

where

$$\mu = \frac{2 - \alpha}{2},$$

$$\beta = \left(\frac{\alpha}{2} \right)^{\alpha/2}.$$

The power series (31) converges slowly. It is therefore numerically useful only for small argument. The maximum difference between the numerical solution and the power series is equal to 4.8×10^{-5} for evaluating the first 150 terms of the series.

In figure 2 the comparison of the numerical results with the power series expansion for small argument and with the asymptote of the analytical solution for large argument (33) is

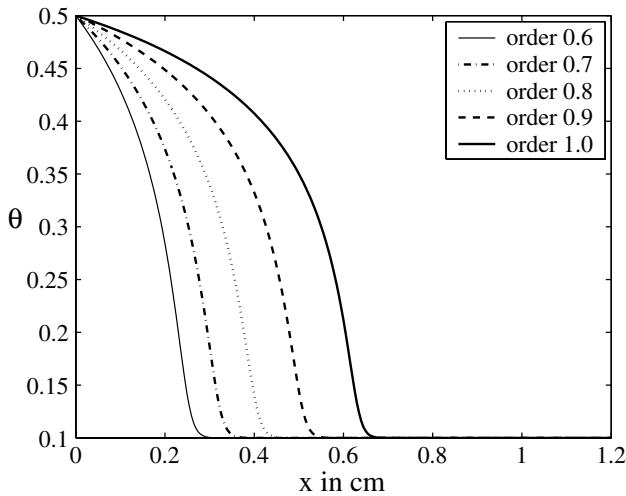


Figure 3. Isochrones of the volumetric moisture content for time equal to 200 min and different orders of derivative.

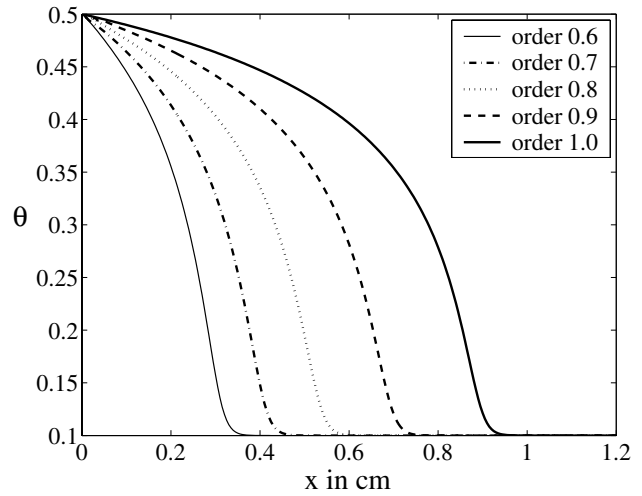


Figure 4. Isochrones of the volumetric moisture content for time equal to 400 min and different orders of derivative.

presented for $\alpha = 0.6$. The asymptote for large argument is plotted for $\xi = x/t^{\alpha/2} \gtrsim 0.1$. In this region the remainder of the asymptotic series becomes smaller than one-tenth of the first term. In order to exhibit the behaviour of the tail the initial value 0.1 has been subtracted and the plot is in logarithmic scale.

5. Numerical results

5.1. Isochrones

Numerical solutions to the nonlinear classical and fractional Richards equations (15) and (16) are shown in figures 3–5. In figure 3 the isochrones of the volumetric moisture content as a function of x for $t = 200$ min and different orders of derivative are plotted. In figures 4 and 5 the isochrones of the volumetric moisture content as a function of x for $t = 400$ min and $t = 600$ min, respectively, and different orders of derivative are shown. From these figures it is observed that the speed of the moisture front decreases with increasing order of the derivative.

5.2. Scaling

As has already been mentioned above, the similarity variable (9) allows to reduce the classical Richards equation into an ordinary differential equation. The fractional Richards equation (16) is invariant under the scaling transformation

$$x \rightarrow \lambda x \text{ and } t \rightarrow \lambda^{2/\alpha} t$$

for any $\lambda > 0$. Thus, $\theta(t, x)$ becomes a function of one variable

$$\theta(t, x) = g_\alpha(x/t^{\alpha/2}) = g_\alpha(\xi). \quad (34)$$

The function g_α is often referred to as a master curve. Inverting (34) gives

$$\xi = \frac{x}{t^{\alpha/2}} = g_\alpha^{-1}(\theta)$$

or equivalently

$$x^2 = (g_\alpha^{-1}(\theta))^2 t^\alpha, \quad (35)$$

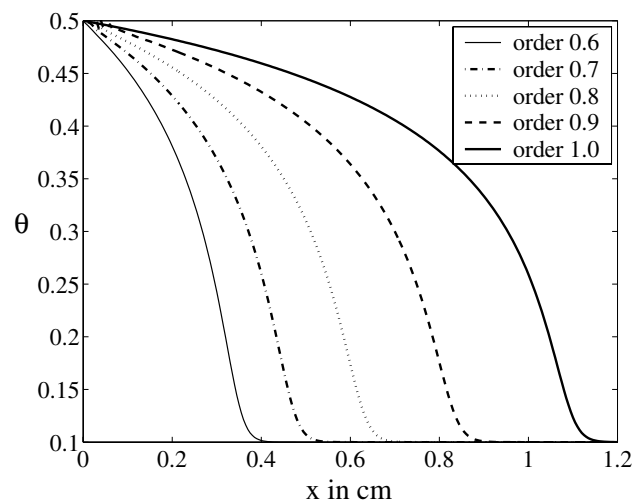


Figure 5. Isochrones of the volumetric moisture content for time equal to 600 min and different orders of derivative.

where g_α^{-1} is a function dependent solely on the volumetric moisture content. This equation can also be written in the form

$$\ln(x^2) = \alpha \ln(t) + 2 \ln(g_\alpha^{-1}(\theta)). \quad (36)$$

In figure 6 the relation between $\log x$ and $\log t$ obtained from the numerical solution is plotted for $\alpha = 0.7, 0.8, 0.9, 1.0$ and $\theta = 0.3$. The numerical results agree with the value of α that was given as a parameter, thereby confirming the scaling property.

5.3. Master curves and cumulative moisture intake

In figure 7 the master curves for the classical and fractional Richards equation are shown. The order used for the fractional Richards equation was chosen to be small, $\alpha = 0.6$, in order to emphasize the differences. For the classical Richards equation the similarity variable is $\xi = x/t^{0.5}$, whereas for the fractional Richards equation with order 0.6 it is $\xi = x/t^{0.3}$.

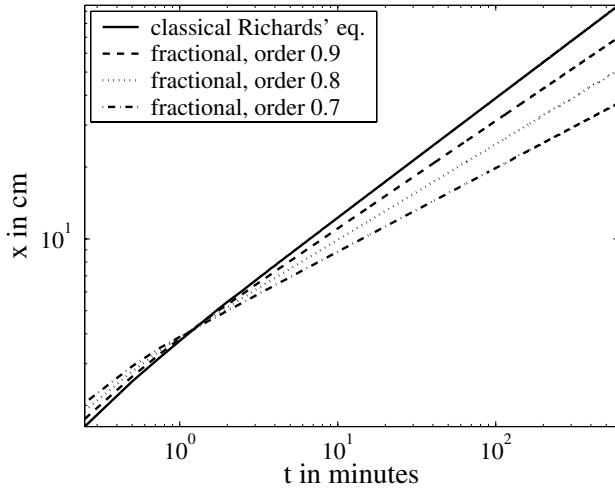


Figure 6. Isosaturation curves for volumetric moisture content $\theta = 0.3$ for different orders of derivative.

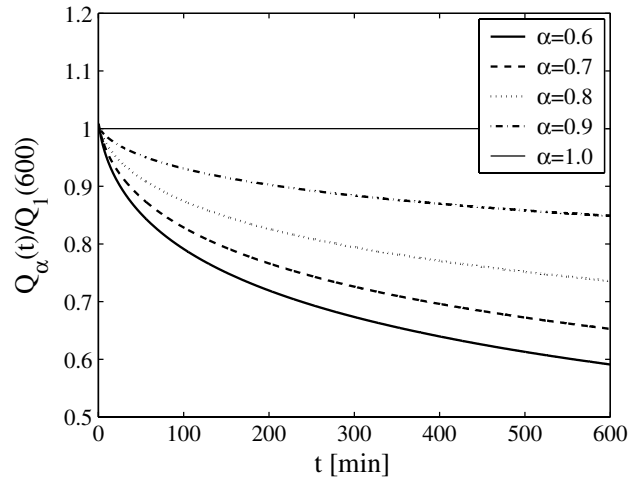


Figure 8. Cumulative moisture intake as a function of time for different orders of derivative.

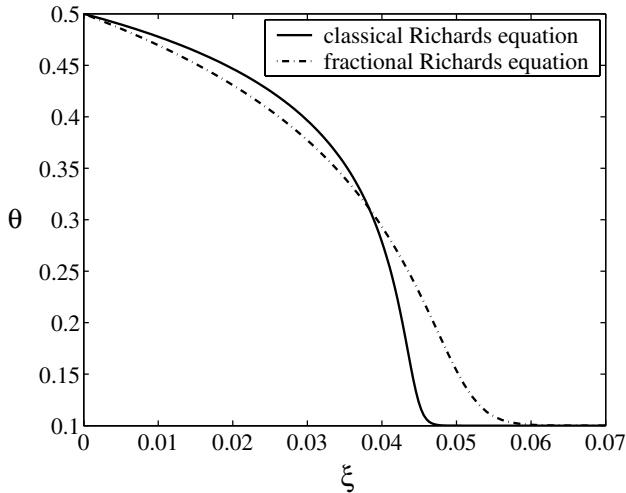


Figure 7. Volumetric moisture content for the nonlinear case of the classical and the fractional of order 0.6 Richards equations as a function of the similarity variable $\xi = x/t^{\alpha/2}$ where $\alpha = 1.0$ and 0.6, respectively.

Figure 8 shows the cumulative moisture intake

$$Q_{\alpha}(t) = \int_0^{\infty} \theta(t, x) dx \quad (37)$$

for different times and different orders of the derivative. The values of the vertical axis in figure 8 denote the ratio to the total intake as evaluated for the classical Richards equation and $t = 600$ min, that is the quantity $Q_{\alpha}(t)/Q_1(600)$. It is notable that after that time even a derivative of order 0.9 results in a significant difference in cumulative moisture intake. For the case mentioned the cumulative moisture intake is less than 85% of the corresponding value for the classical Richards equation.

5.4. Comparison with experimental results

In [12] experiments on white siliceous brick samples were performed and the similarity variable was found to be $\xi = x/t^{0.43}$. In figure 9 the experimental data from [12] in

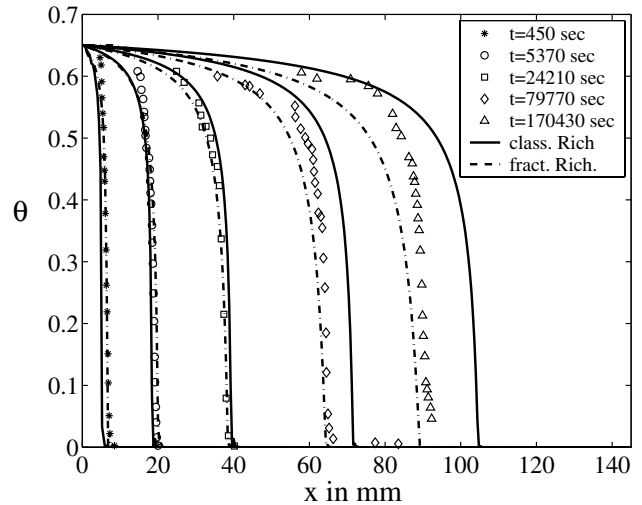


Figure 9. Experimental data for white siliceous brick (data taken from [12]) and corresponding numerical isochrones.

the form of isochrones are replotted. In the same figure the isochrones resulting from the classical and the fractional Richards equation for order $\alpha = 0.86$ are shown. For both cases the same function was used for the diffusivity, namely a function of the form

$$C(\theta) = C_0 \left(1 - A \frac{\theta}{\theta_s}\right)^{2-4/\alpha} \left[\frac{1-A}{A} \log \left(1 - A \frac{\theta}{\theta_s}\right) + \frac{\theta}{\theta_s} \right], \quad (38)$$

where A and θ_s are fit parameters, as suggested in [12]. For each case the constant C_0 was selected to optimize the fit of the numerical to the experimental results. As can be seen from the figure it is not possible to draw a firm conclusion. While the experimental data seem more consistent with the fractional approach, they are too uncertain to be conclusive evidence for the value of α . In order to reach a definite conclusion better experimental data are necessary.

6. Summary

In the present work a fractional diffusion equation was proposed to model moisture transport processes in porous media, whose time scaling deviates systematically from the classical diffusive scaling. The fractional Richards equation was solved numerically. The numerical algorithm was validated by comparison with analytical results for the corresponding linear equations. The fractional scaling that was expected to arise from the solution of the fractional Richards equation was confirmed. The master curves and the cumulative moisture intakes for different orders of the derivative were compared. The numerical results for saturation profiles were compared with experimental data. It would be interesting to include a comparison of the fractional time model discussed above to other generalizations of the Richards equation. Unfortunately, such comparisons must be left for future work due to the limited resources available for this project.

Acknowledgments

This paper is a partial result of the Project Puthagoras II/EPEAEK II. The Project is co-funded by the European Social Fund (75%) and National Resources (25%). One of us (RH) acknowledges support from the Deutsche Forschungsgemeinschaft.

References

- [1] Muskat M 1937 *The Flow of Homogeneous Fluids through Porous Media* (New York: McGraw Hill)
- [2] Hilfer R 1996 Transport and relaxation phenomena in porous media *Advances in Chemical Physics* vol XCII p 299
- [3] Dullien F A L 1992 *Porous Media—Fluid Transport and Pore Structure* (San Diego, CA: Academic)
- [4] Hilfer R 1998 Macroscopic equations of motion for two phase flow in porous media *Phys. Rev. E* **58** 2090
- [5] Hilfer R and Besserer H 2000 Macroscopic two phase flow in porous media *Physica B* **279** 125
- [6] Hilfer R 2006 Capillary pressure, hysteresis and residual saturation in porous media *Physica A* **359** 119
- [7] Hilfer R 2006 Macroscopic capillarity and hysteresis for flow in porous media *Phys. Rev. E* **73** at press
- [8] Richards L A 1931 Capillary conduction of liquids through porous mediums *Physics* **1** 318–333
- [9] de Marsily G 1986 *Quantitative Hydrogeology—Groundwater Hydrology for Engineers* (San Diego, CA: Academic)
- [10] Taylor S C, Hoff W D, Wilson M A and Green K M 1999 Anomalous water transport properties of Portland and blended cement-based materials *J. Mater. Sci. Lett.* **18** 1925–27
- [11] Küntz M and Lavalée P 2001 Experimental evidence and theoretical analysis of anomalous diffusion during water infiltration in porous building materials *J. Phys. D: Appl. Phys.* **34** 2547–54
- [12] El Abd A El-G and Milczarek J J 2004 Neutron radiography study of water absorption in porous building materials: anomalous diffusion analysis *J. Phys. D: Appl. Phys.* **37** 2305–13
- [13] Gerolymatou E, Vardoulakis I and Hilfer R 2005 Simulating the saturation front using a fractional diffusion model *Proc. GRACM05 Int. Congr. on Computational Mechanics, Limassol 2005* ed G Georgiou *et al* (Athens: GRACM) pp 653–60
- [14] Pachepsky Y, Timlin D and Rawls W 2003 Generalized Richard's equation to simulate water transport in unsaturated soils *J. Hydrol.* **272** 3–13
- [15] Jacques Y, Šimůnek J and Feyen J 2002 Calibration of Richards' and convection-dispersion equations to field-scale water flow and solute transport under rainfall conditions *J. Hydrol.* **259** 15–31
- [16] Lewandowska J and Auriault J-L 2002 Modelling of unsaturated water flow in soils with highly permeable inclusions *C. R. Mecanique* **332** 91–6
- [17] Van Dam J C and Feddes R A 2000 Numerical simulation of infiltration, evaporation and shallow groundwater levels with the richards equation *J. Hydrol.* **233** 72–85
- [18] Hall C 1989 Water sorptivity of mortars and concretes: a review *Mag. Concrete Res.* **41** 51–61
- [19] Carmeliet J, Hens H, Roels S, Adan O, Brocken H, Cerny R, Pavlic Z, Hall C, Kumaran K and Pel L 2004 Determination of the liquid water diffusivity from transient moisture transfer experiments *J. Therm. Envelope Build. Sci.* **27** 277–305
- [20] Lockington D, Parlange J Y and Dux P 1999 Sorptivity and the estimation of water penetration into unsaturated concrete *Mater. Struct.* **32** 342–7
- [21] Gardner W R and Mayhugh M S 1958 Solutions and tests of the diffusion equation for the movement of water in soil *Soil Sci. Soc. Am. Proc.* **22** 197–201
- [22] Raats P A C 2001 Developments in soil-water physics since the mid 1960 *Geoderma* **100** 355–87
- [23] Philip J R 1969 Theory of infiltration *Adv. Hydroscl.* **5** 215–96
- [24] Hillel D 1980 *Applications of Soil Physics* (New York: Academic)
- [25] Hilfer R 2000 Fractional time evolution *Applications of Fractional Calculus in Physics* (Singapore: World Scientific) chapter 2 pp 87–130
- [26] Samko S G, Kilbas A A and Marichev O I 1993 *Fractional Integrals and Derivatives: Theory and Applications* (Switzerland: Publishers S.A.)
- [27] Hilfer R 2000 Fractional diffusion based on Riemann–Liouville fractional derivatives *J. Phys. Chem. B* **104** 3914
- [28] Hilfer R and Anton L 1995 Fractional master equations and fractal time random walks *Phys. Rev. E* **51** R848–51
- [29] Diethelm K and Freed A D 1999 On the solution of nonlinear fractional-order differential equations used in the modelling of viscoplasticity *Scientific Computations in Chemical Engineering II-Computational Fluid Dynamics, Reaction Engineering, and Molecular properties* (Heidelberg: Springer) pp 217–24
- [30] Rheinboldt W C 1978 Numerical methods for a class of finite dimensional bifurcation problems *SIAM J. Numer. Anal.* **15** 1–11
- [31] Strang G and Fix G C 1973 *An Analysis of the Finite Element Method* (Englewood Cliffs, NJ: Prentice Hall)
- [32] Braaksma B L J 1964 Asymptotic expansions and analytic continuations for a class of Barnes integrals *Compos. Math.* **15** 239–341